Phytomedicine 96 (2022) 153908

Contents lists available at ScienceDirect

Phytomedicine

journal homepage: www.elsevier.com/locate/phymed

Astragaloside IV promotes the angiogenic capacity of adipose-derived mesenchymal stem cells in a hindlimb ischemia model by FAK phosphorylation via CXCR2

Weiyi Wang [1], Zekun Shen [1], Yanan Tang, Bingyi Chen, Jinxing Chen, Jiaxuan Hou, Jiayan Li, Mengzhao Zhang, Shuang Liu, Yifan Mei, Liwei Zhang, Shaoying Lu [*]

Department of Vascular surgery, The First Affiliated Hospital of Xi'an Jiaotong University, Xi'an, China

ARTICLE INFO

Keywords:
Angiogenesis
Mesenchymal stem cells
Astragaloside IV
Ischemic hindlimb
Chemokine

ABSTRACT

Background: Therapeutic angiogenesis by transplantation of autologous/allogeneic adipose stem cells (ADSCs) is a potential method for the treatment of critical limb ischemia (CLI). However, the therapeutic efficiency is limited by poor viability, adhesion, migration and differentiation after cell transplantation into the target area. Astragaloside IV (AS-IV), one of the main active components of Astragalus, has been widely used in the treatment of ischemic diseases and can promote cell proliferation and angiogenesis. However, there is no report on the effect of AS-IV on ADSCs and its effect on hindlimb ischemia through cell transplantation.

Purpose: The purpose of this study was to elucidate that AS-IV pretreatment enhances the therapeutic effect of ADSC on critical limb ischemia, and to characterize the underlying molecular mechanisms.

Methods: ADSCs were obtained and pretreated with the different concentration of AS-IV. *In vitro*, we analyzed the influence of AS-IV on ADSC proliferation, migration, angiogenesis and recruitment of human umbilical vein endothelial cells (HUVECs) and analyzed the relevant molecular mechanism. *In vivo*, we injected drug-pretreated ADSCs into a Matrigel or hindlimb ischemia model and evaluated the therapeutic effect by the laser Doppler perfusion index, immunofluorescence, and histopathology.

Results: In vitro experiments showed that AS-IV improved ADSC migration, angiogenesis and endothelial recruitment. The molecular mechanism may be related to the upregulation of CXC receptor 2 (CXCR2) to promote the phosphorylation of focal adhesion kinase (FAK). *In vivo*, Matrigel plug assay showed that ADSCs pretreated with AS-IV have stronger angiogenic potential. The laser Doppler perfusion index of the hindlimbs of mice in the ADSC/AS-IV group was significantly higher than the laser Doppler perfusion index of the hindlimbs of mice of the ADSC group and the control group, and the microvessel density was significantly increased.

Conclusion: Our results demonstrate that AS-IV pretreatment of ADSC improves their therapeutic efficacy in ameliorating severe limb exclusion symptomology through CXCR2 induced FAK phosphorylation, which will bring new insights into the treatment of severe limb ischemia.

Introduction

CLI, an ischemic disease that occurs in the extremities, is a serious form of peripheral arterial disease that can cause resting pain, ulcers, and tissue necrosis (Campia et al., 2019). Patients suffering from CLI always have poor physical function and have a very high risk of amputation. For the treatment of CLI, surgical methods (such as arterial reconstruction and arterial bypass) to increase blood perfusion were

Abbreviations: ADSC, adipose stem cell; AS-IV, astragaloside iv; CLI, critical limb ischemia; CM, conditioned medium; CXCR2, CXC receptor 2; DAPI, 4′′, 6-diamidino-2-phenylindole; DMEM, Dulbecco's modified Eagle's medium; DMEM/F-12, Dulbecco's modified Eagle's medium F-12; DMSO, dimethyl sulfoxide; FAK, focal adhesion kinase; HIF-1α, hypoxia-inducible factor-1α; HUVEC, human umbilical vein endothelial cell; Matrigel, matrix gel; MSC, mesenchymal stem cell; MTT, 3- (4,5-dimethylthiazole-2-yl) -2,5-diphenyltetrazolium bromide; PBS, phosphate buffered saline; PMSF, Phenylmethylsulfonyl fluorid; PVDF, polyvinylidene fluoride; PXN, paxillin; TBST, Tris buffered saline with Tween; VEGF, vascular endothelial growth factor.

* Corresponding author at: 710061, China
E-mail address: robertlu@mail.xjtu.edu.cn (S. Lu).

[1] These authors contributed equally to this work

https://doi.org/10.1016/j.phymed.2021.153908
Received 9 November 2021; Received in revised form 13 December 2021; Accepted 21 December 2021
Available online 30 December 2021

usually used in the past. However, more than 55% of patients could not receive surgical treatment because of high surgical risk or adverse vascular anatomy (Beltran-Camacho et al., 2021), and their quality of life was seriously affected.

In the past 20 years, the use of cytotherapy to rebuild blood vessels and improve limb blood perfusion has become a new treatment for CLI, especially for patients who are not suitable for surgical or interventional surgery. As early as 2002, autologous mononuclear bone marrow cells were transplanted into patients with limb ischemia to achieve therapeutic angiogenesis (Tateishi-Yuyama et al., 2002). Then, various kinds of mesenchymal stem cells (MSCs) were extracted from tissues such as bone marrow, adipose tissue (Zuk et al., 2002), dental pulp (Potdar and Jethmalani, 2015), skin (Orciani and Di Primio, 2013), umbilical cord, and endometrium (Li et al., 2015). MSCs have been postulated and determined to promote angiogenesis through their paracrine effects, differentiation effects (myogenic differentiation and endothelial differentiation), and immunomodulatory effects (Liew and O'Brien, 2012). Among them, ADSCs are more widely studied and used because they include a larger angiogenic response through upregulating cell proliferation (Hutchings et al., 2020; Lu et al., 2018) and are easier to extract and autotransplant. The problem that researchers are currently facing is how to improve the therapeutic effect of cell transplantation. In addition to improving the retention of ADSCs in ischemic tissues, improving the migration ability and paracrine function of ADSCs can also produce important benefits (Min et al., 2018).

Astragaloside IV, a saponin purified from Astragalus, has been widely used for a long time in traditional Chinese medicine to treat ischemic diseases. Numerous studies have shown that Astragalus has positive effects, such as protecting hypoxic myocardial cells (Cheng et al., 2019), promoting angiogenesis (Feng et al., 2017), inhibiting muscle damage (Jiang et al., 2020). The potential mechanisms include activation of the PI3K/Akt signaling pathway, JAK2/STAT3 and ERK1/2 signaling pathways (Wang et al., 2013), AMPK signaling pathway (Xu et al., 2018) and overexpression of vascular endothelial growth factor (VEGF) and hypoxia-inducible factor-1α (HIF-1α) (Zhang et al., 2011).

Therefore, in this study, we pretreated ADSCs with AS-IV, analyzed their activity, proliferation, migration and effect on angiogenesis, and tried to find out the molecular mechanism of these effects. Then, we transplanted AS-IV-treated ADSCs into a Matrigel to evaluate its angiogenic potential and into ischemic hindlimb mice to evaluate the therapeutic effect by the laser Doppler perfusion index, histopathology, and immunofluorescence.

Methods

Reagents

Chemical reagents AS-IV (molecular formula: $C_{14}H_{68}O_{14}$; molecular weight: 784.97 g/mol; purity ≥ 98.0%; #HY-N0431), SB225002 (#HY-16711) and AMD3100 (#HY-10046) were purchased from MedChemExpress (Monmouth Junction, NJ, USA), and PF573228 (#T2001) was purchased from TargetMol (Boston, MA, USA). According to the instructions, dry powders of AS-IV, SB225002 and PF573228 were dissolved and diluted with dimethyl sulfoxide (DMSO), and dry powders of AMD3100 were dissolved and diluted with ethanol.

Isolation of ADSCs

Human adipose tissue was obtained from the subcutaneous fat of the upper arm and abdomen of a 30-year-old healthy female donor (The First Affiliated Hospital of Xi'an Jiaotong University, China) through liposuction. To extract ADSCs, adipose tissue was cut into small pieces, placed in a centrifuge tube, rinsed with phosphate buffered saline (PBS) and centrifuged (1000 rpm, 5 min). The lower liquid was aspirated, the adipose tissue was digested at 37 °C for 40 min using a digestion solution containing 0.2% collagenase I (#SCR103, Sigma–Aldrich, St Louis, MO, USA), and the centrifuge tube was shaken several times during digestion. Then, an equal volume of DMEM/F-12 medium containing 10% fetal bovine serum was added for neutralization, pipetted for 5 min and centrifuged (1500 rpm, 10 min). After centrifugation, the lowermost cell-containing mixed liquid was aspirated and centrifuged twice (1000 rpm, 5 min). Culture medium was added to resuspend the cells, filtered with a 200-mesh cell strainer, and inoculated into a 60 mm cell culture dish. The medium was changed every other day until the cells reached 80%–90% confluence. The cells can be harvested for expansion and cryopreservation.

Cell culture

HUVECs were purchased from American Type Culture Collection (ATCC) (#PCS-100–013, ATCC, Manassas, VA, USA), and the cells were cultured in Dulbecco's modified Eagle's medium (DMEM) (#A4192101, Gibco, Grand Island, NY, USA) supplemented with 10% fetal bovine serum (#900–108, Gemini, Woodland, CA, USA) and 1% antibiotic-antimycotic (#SV30010, HyClone, Logan, UT, USA). ADSCs were cultured in Dulbecco's modified Eagle's medium F-12 (DMEM/F-12) (#A4192001, Gibco) supplemented with 10% fetal bovine serum and 1% antibiotic-antimycotic. Cells were incubated at 37 °C in a 5% CO_2 humidified incubator. ADSCs used in this study were less than 6 passages (P6).

Flow cytometry

Trypsin (#SH30042.01, HyClone) digested the cells and resuspended with PBS to a concentration of 1×10^6 cells/100 μl. The samples were mixed with anti-human CD29-FITC (#11–0299–41, eBioscience, San Diego, CA, USA), CD44-PE (#12–0441–81, eBioscience), CD90-FITC (#11–0909–41, eBioscience), CD105-APC (#17–1057–41, eBioscience), CD34-APC (#17–0349–41, eBioscience), CD45-PE (#12–0456–41, eBioscience). The cell suspension was incubated with flow cytometry antibody (diluted 1:20) at 4 °C in the dark for 30 min. Finally, a FACSCalibur™ flow cytometer (BD Biosciences, Franklin Lakes, NJ, USA) was used to analyze the stained cells. FlowJo 10 (BD Biosciences) software was used to analyze the data. The experiment was repeated three times.

MTT assay

ADSCs in logarithmic growth phase were treated with the indicated treatment method, and then the cell viability was detected by 3-(4,5-dimethylthiazole-2-yl)-2,5-diphenyltetrazolium bromide (MTT) (#57360–69–7, Sigma–Aldrich). ADSCs were suspended at a concentration of 3×10^4 cells/ml and seeded in a 96-well plate at 200 μl per well. After incubating for a specific time in the cell culture incubator, 20 μl of MTT was added to 180 μl of complete medium per well. After four hours, the liquid was removed from the 96-well plate, 150 μl of DMSO was added, and the plate was shaken for 10 min. The absorbance was measured at 490 nm by an ELISA reader (Bio–Rad, Hercules, CA, USA). The experiment was repeated three times.

Preparation of conditioned medium

A total of 5×10^5 cells were inoculated into a 10 cm cell culture dish and grown in DMEM/F-12 supplemented with 10% fetal bovine serum and 1% antibiotic-antimycotic and different concentrations of AS-IV for 48 h until the cells reached approximately 80% confluence. Then, the medium was replaced with FBS-free medium and incubated for 48 h. Then, the medium was collected and centrifuged, conditioned medium (CM) was obtained and used for this study. For the inhibitor group, we added an appropriate concentration of inhibitor (SB225002 or PF573228) 1 hour before adding AS-IV, and the subsequent treatment was the same as described above.

Wound healing assay

ADSCs or HUVECs were inoculated in 6-well plates and grown to a 90% fusion rate. Wounds were generated on the cell monolayer using a 200 μl sterile pipette tip, and the fragments were washed with PBS. For ADSCs, the medium were changed to serum-free medium containing different concentrations of AS-IV or inhibitors (SB225002 or PF573228); for HUVECs, the medium were change to a different group of CM. After 24 h, the migration of cells to the wound was observed by inverted microscopy at different time points. Under the condition of 100 times magnification, regions were randomly selected in each well, and the areas between the two cell fronts were quantified. The experiment was repeated three times.

Transwell migration assay

Migration assays were performed in a Boyden chamber (#MCEP24H48, Millipore, Darmstadt, Germany) with a pore size of 8 μm to evaluate the migratory ability of ADSCs and the recruitment of HUVECs. For migration assays, 1.5×10^4 pretreated ADSCs were seeded into a chamber in a 24-well plate, the cells were suspended in 100 μl serum-free medium in the upper chamber, and 600 μl medium containing 10% FBS was added to the lower chamber. For recruiting assays, 1.5×10^4 HUVECs were inoculated in the upper chamber, and different CMs were added to the lower chamber. After 24 h, the chamber was washed with PBS 3 times, fixed with 4% paraformaldehyde for 15 min, and stained with 0.1% crystal violet for 15 min. Then, the upper part of the filter was wiped and inverted under a light microscope (200 times magnification) to observe the visible cell count in 3 random visual fields. The experiment was repeated three times.

qRT–PCR

According to the manufacturer's instructions, total RNA was isolated from ADSCs cells using RNAfast 200 reagents (#220010, Feijie Biotechnology, Shanghai, China), quantified by absorbance at 260 nm and reverse-transcribed to complementary DNA using a Prime Script RT–PCR kit (#RR036A, Takara Bio, Dalian, China). cDNA was amplified to detect the expression of specific genes using a CFX96 Real-Time PCR system (Bio–Rad) with SYBR-Green PCR Master Mix (#RR820A, Takara Bio). The sequences of the primer pairs are shown in Table 1. mRNA expression levels were assessed by the $2^{-\Delta\Delta Ct}$ method. GAPDH was used for standardization.

Western blot assay

After treatment, ADSCs were washed 3 times with PBS, and the total protein was separated with RIPA lysis buffer (#P0013B, Beyotime, Shanghai, China) containing protease inhibitor, phosphatase inhibitor and 0.1 M Phenylmethylsulfonyl fluorid (#ST506, PMSF, Beyotime). Cells were centrifuged at 12,000 g at 4 °C for 20 min, and cell lysates containing total cell proteins were collected and quantified by the BCA Protein Assay Kit (#23225, Thermo Fisher Scientific, Waltham, MA, USA). The processed protein samples were subjected to SDS-polyacrylamide gel electrophoresis (8%–12%), and then transferred to a polyvinylidene fluoride (PVDF) membrane. After sealing with 5% skim milk at room temperature for 1 hour to block the nonspecific binding sites, the membrane was incubated with the primary antibody (diluted 1:1000) at 4 °C overnight. After washing with Tris Buffered Saline with Tween (TBST) 3 times, the membrane and peroxidase-coupled secondary antibody were incubated at room temperature for 1 hour. Finally, protein expression was detected by an ECL chemiluminescence detection system (Bio–Rad). The antibodies used in the experiment were as follows: CXCR2 (#ab225732), CXCR4 (#ab181020), p-PXN (Y118) (#ab109547), t-PXN (#ab32084) were purchased from Abcam (Cambridge, United Kingdom), p-FAK (Tyr397) (#8556), t-FAK (#3285) and β-Catenin (#8480) were purchased from Cell Signaling Technology (Boston, MA, USA).

Table 1
PCR primers.

NCBI Gene ID	Gene	Primers (5 ' −3 ')
3577	*CXCR1*	F: CTGACCCAGAAGCGTCACTTG
		R: CCAGGACCTCATAGCAAACTG
3579	*CXCR2*	F: CCTGTCTTACTTTTCCGAAGGAC
		R: TTGCTGTATTGTTGCCCATGT
7852	*CXCR4*	F: ACTACACCGAGGAAATGGGCT
		R: CCCACAATGCCAGTTAAGAAGA
2919	*CXCL1*	F: CCCAAACCGAAGTCATAGCC
		R: ATCCGCCAGCCTCTATCACA
2920	*CXCL2*	F: TCCAAGAAAGGGCGAAATAAGG
		R: TGCAGCTCTATCTGAATGTCTGT
2921	*CXCL3*	F: CGCCCAAACCGAAGTCATAG
		R: GCTCCCCTTGTTCAGTATCTTTT
6374	*CXCL5*	F: AGCTGCGTTGCGTTTGTTTAC
		R: TGGCGAACACTTGCAGATTAC
6372	*CXCL6*	F: AGAGCTGCGTTGCACTTGTT
		R: GCAGTTTACCAATCGTTTTGGGG
5473	*CXCL7*	F: GTAACAGTGCGAGACCACTTC
		R: CTTTGCCTTTCGCCAAGTTTC
3576	*CXCL8*	F: TTTTGCCAAGGAGTGCTAAAGA
		R: AACCCTCTGCACCCAGTTTTC
6387	*CXCL12*	F: ATTCTCAACACTCCAAACTGTGC
		R: ACTTTAGCTTCGGGTCAATGC
2247	*bFGF*	F: AGAAGAGCGACCCTCACATCA
		R: CGGTTAGCACACACTCCTTTG
7422	*VEGF*	F: AGGGCAGAATCATCACGAAGT
		R: AGGGTCTCGATTGGATGGCA
2597	*GAPDH*	F: GGAGCGAGATCCCTCCAAAAT
		R: GGCTGTTGTCATACTTCTCATGG

Matrigel tube formation assay

Fifty microliters of LDEV-free basement membrane matrix gel (Matrigel) (#356234, Corning Incorporated, Corning, NY, USA) was spread on the bottom of a 96-well plate at 4 °C, and placed at 37 °C until Matrigel solidified. HUVECs were suspended at a concentration of 1.5×10^4 cells per 150 μl in each kind of CM and inoculated onto a previous Matrigel-coated 96-well plate. After 4 h of incubation, the field of view was randomly photographed, and the number of lumens formed by each sample and the length of the tube were measured with ImageJ software (National Institutes of Health, Bethesda, MD, USA). The experiment was repeated three times.

Matrigel plug in vivo assay

All male C57BL/6 mice used in this study were approved by the ethics committee of The First Affiliated Hospital of Xi'an Jiaotong University, China (Approval number: 2021–1568, Approval date: May 6, 2021). To assess the *in vivo* angiogenic potential of cells, Matrigel plug assays were performed as described in previous literature (Min et al., 2018). Briefly, 6- to 8-week-old C57BL/6 mice were anesthetized with isoflurane, 5×10^4 ADSCs were suspended in 50 μl PBS and mixed with 450 μl Matrigel, and the cells were subcutaneously transplanted into mice. After 2 weeks, the mice were euthanized, and Matrigel plugs were collected. Half of each plug was used for section staining, and the other half was used to measure the level of hemoglobin by the Drabkin kit (#D5941, Sigma–Aldrich). The experiment was repeated 3 times.

Ischemic hind limb mice model and cell injection

An ischemic hindlimb modle was induced in which 18 male C57BL/6 mice aged 6–8 weeks were randomly divided into three groups, with each group containing 6 mice (Limbourg et al., 2009; Min et al., 2018). Each mouse was anesthetized with isoflurane and its left femoral artery was ligated and resected. ADSCs were pretreated with 20 μM or 40 μM

AS-IV for 48 h. A total of 1×10^6 cells or PBS were intramuscularly transplanted into the ischemic hindlimb area after surgery. A laser Doppler perfusion imager (Moor Instrements, Devon, United Kingdom) was used to measure blood perfusion in the hind limbs at 0, 3, 7, 14, and 21 days after the operation. The left-to-right ratio (l/R) was used to indicate the relative blood perfusion rate of each mouse's left hind limb. The mice were euthanized 4 weeks after the operation, and their left gastrocnemius muscle was collected to make paraffin-embedded sections for immunohistochemistry and immunofluorescence analysis.

H&E staining

Formalin-fixed Matrigel plugs or gastrocnemius specimens were embedded in paraffin. The slides were prepared from 6 μm thick sections. For histological analysis, hematoxylin (#H3136, Sigma–Aldrich) and eosin (#212954, Sigma–Aldrich) staining were applied. The experiment was repeated three times.

Immunofluorescence staining

The slices were dewaxed and rehydrated. Endogenous peroxidase was inactivated with 10% hydrogen peroxide for 10 min. The antigen was recovered by pepsin at 37 °C for 10 min. The sections were blocked in 5% BSA for 30 min and then mixed with 1:500 CD31 antibody (#ab28364; Abcam) and incubated at room temperature for 1 hour. After washing, the slices were incubated with the secondary antibody for 1 h at room temperature, and the nuclei were stained with 4′, 6-diamidino-2-phenylindole (DAPI) (#D9542, Sigma–Aldrich) for 5 min and sealed with glycerol. The stained image was captured under a positive fluorescence microscope (Olympus, Tokyo, Japan), and the proportion of CD31+ area in each photo was measured by ImageJ software. The experiment was repeated three times.

Statistical analyses

Statistical analyses were conducted using Student's *t*-test for comparisons of 2 groups, and graphs were drawn by using GraphPad Prism 7.0 (San Diego, CA, USA). The data are expressed as the mean ± SD of three independent experiments. $p < 0.05$ indicated statistically significant.

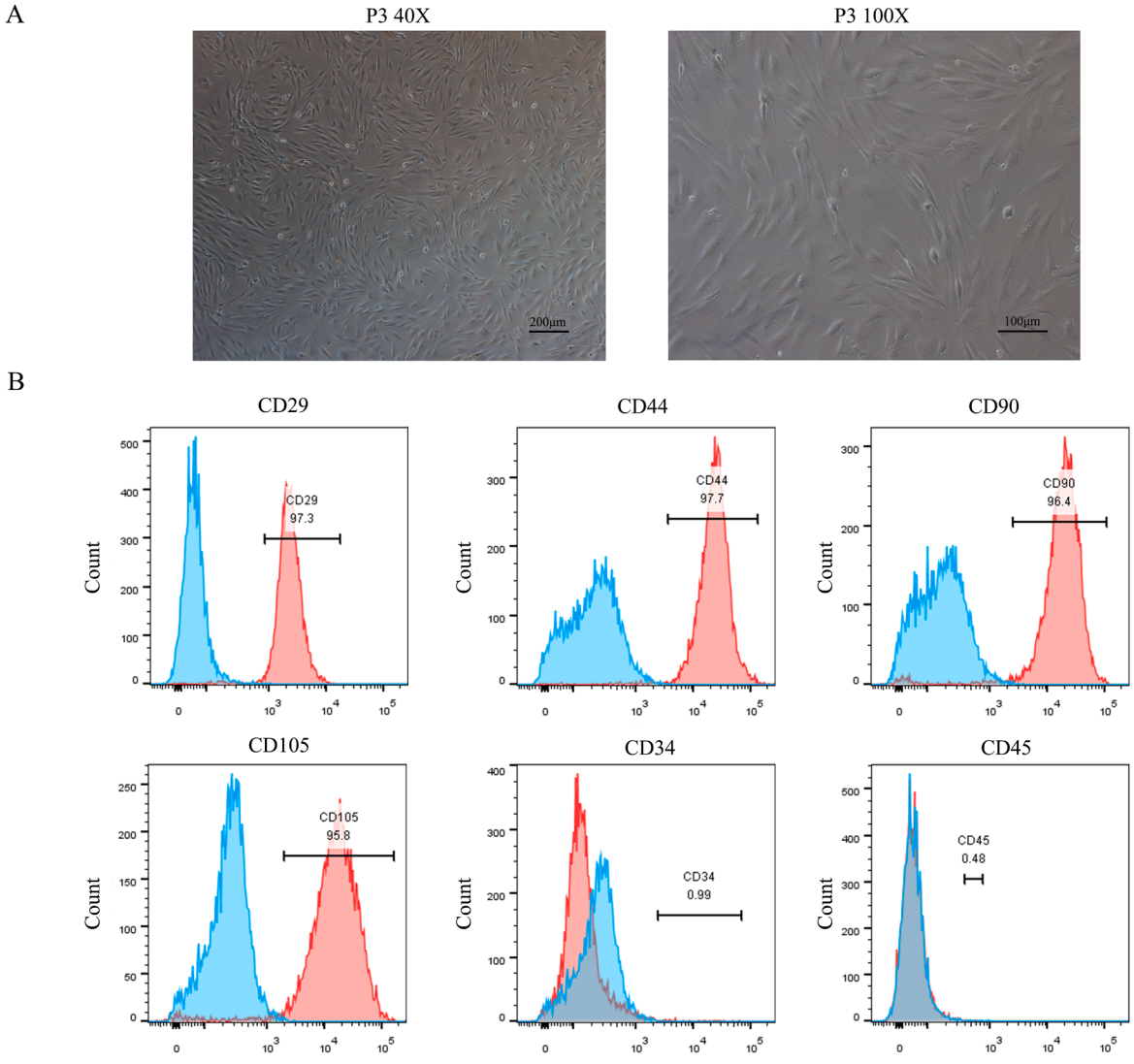

Fig. 1. Characterization and flow cytometry analysis of ADSCs. (A) Passage 3 ADSCs under 40 × optical lenses (left) and 100 × optical lenses (right). Cells showed a fibroblast-like shape and were distributed in a whirlpool shape. (B) Flow cytometry analysis of the ADSCs surface markers CD29, CD44, CD90 and CD105. Hematopoietic cell-specific surface antigen CD34 and leukocyte surface marker CD45 were also analyzed. Blue peaks represent matched negative controls. The experiment was repeated three times.

Results

Characterization and identification of ADSCs

Monocytes isolated from healthy human adipose tissue were cultured and passaged in a Petri dish, and the cells were in the form of a fibroblast-like spindle and grew in a whirlpool (Fig. 1A). To confirm the identity of ADSCs, flow cytometry analysis was used to detect the expression of cell surface markers. The results showed that the representative markers of mesenchymal stem cells (CD29, CD44, CD90, CD105) were positively expressed, whereas the surface markers of hematopoietic stem cells CD34 was weakly positive expressed and the leukocyte surface markers CD45 were negatively expressed. The isolated cells were confirmed to be adipose-derived mesenchymal stem cells (Fig. 1B).

AS-IV enhance ADSCs migration

Different doses (20–160 μM) of AS-IV were used to treat ADSCs (DMSO as a solvent control) for 48 h, and the MTT assay was used to detect cell proliferation. As shown in Fig. 2B, low concentrations of AS-IV had little effect on the proliferation of ADSCs. In contrast, excessive concentrations of AS-IV (80 μM and 160 μM) can inhibit the growth of ADSCs. However, the scratch experiment showed that, within the appropriate range, AS-IV promoted the migration of ADSCs in a concentration-dependent manner (Fig. 2C), and the Transwell experiment confirmed this phenomenon (Fig. 2D).

AS-IV promotes the recruitment of HUVECs and tube formation

We extracted the CM of ADSCs treated under different conditions and acted on vascular endothelial cells. Wound healing assays and Transwell assays showed that the CM of ADSCs pretreated with AS-IV promoted the migration of HUVECs (Fig. 3A and 3B), especially in AS-IV (40 μM) group, that is, promoted the recruitment of HUVECs by ADSCs. The tube formation experiment (Fig. 3C) also showed that ADSCs pretreated with 40 μM AS-IV had a larger effect on angiogenesis, as reflected by the number of tubes formed and the total length of the tubes.

AS-IV mediates the expression of CXCR2 and phosphorylation of FAK in a concentration-dependent manner

Based on the promotion of ADSCs migration ability and endothelial cell recruitment by AS-IV, we focused on the chemokine system. Previous studies have shown that CXC chemokines not only play an important role in cell migration but are also important in arteriogenesis and tissue ischemia repair. Therefore, we used RT–PCR to screen angiogenesis related CXC chemokine ligands and their receptors after treatment of ADSC (Fig. S1). The results showed that the expression of CXCR2 at the RNA level and protein level increased in a concentration dependent manner in ADSCs treated with AS-IV (Fig. 4A and 4B), and the CXCR4 level also increased but was excluded in the follow-up verification (Fig. S2). At the same time, FAK and paxillin (PXN) were also activated, the expression of β-Catenin was increased (Fig. 4C), and the mRNA expression of the angiogenesis-related factors bFGF and VEGF was increased (Fig. 4D).

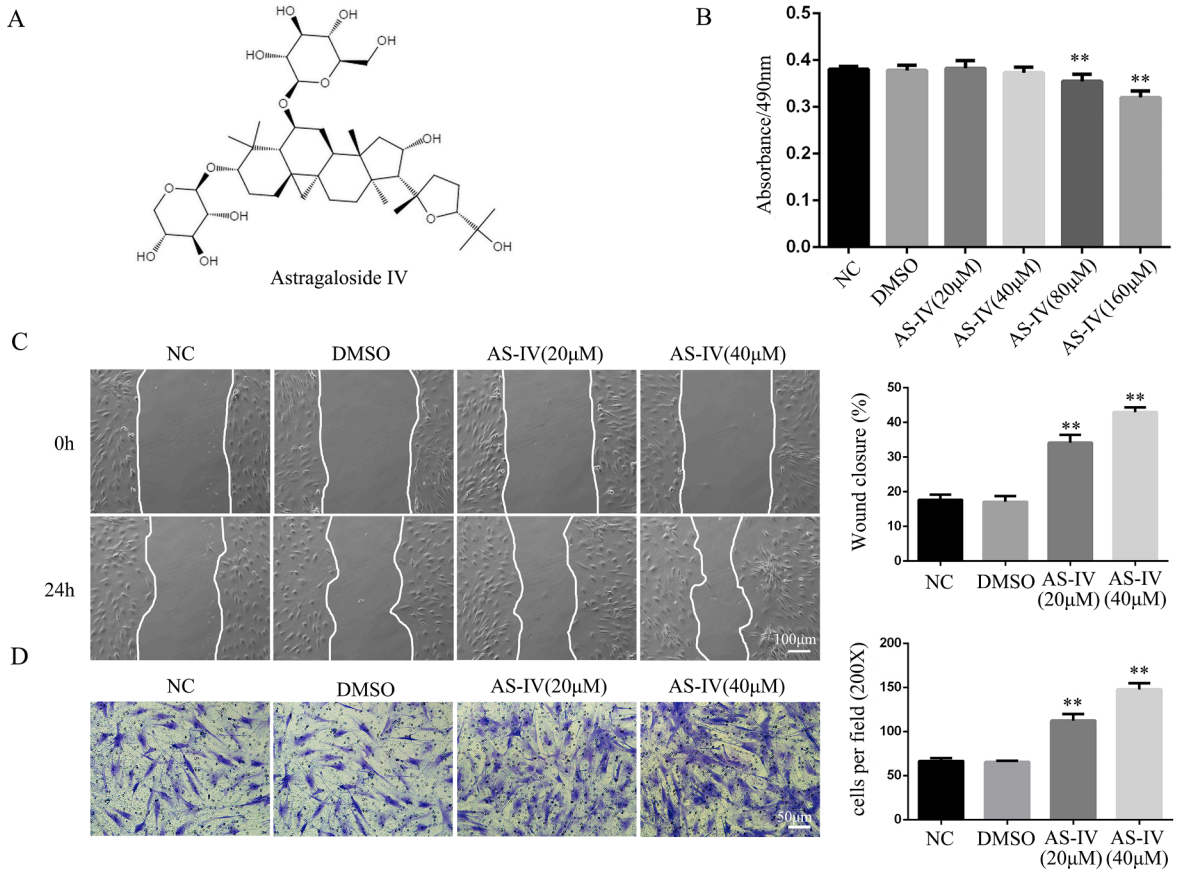

Fig. 2. Effects of AS-IV on ADSC viability and migration. (A) The chemical structure of AS-IV. (B) ADSC growth after treatment with different concentrations of AS-IV for 48 h was assessed by MTT. The migration ability of ADSCs after treatment with AS-IV at different concentrations for 48 h was assessed by wound healing assay (C) and Transwell assay (D), and the quantitative results are shown on the right side, ** $p < 0.01$ *vs.* the NC group. All the experiments were repeated three times.

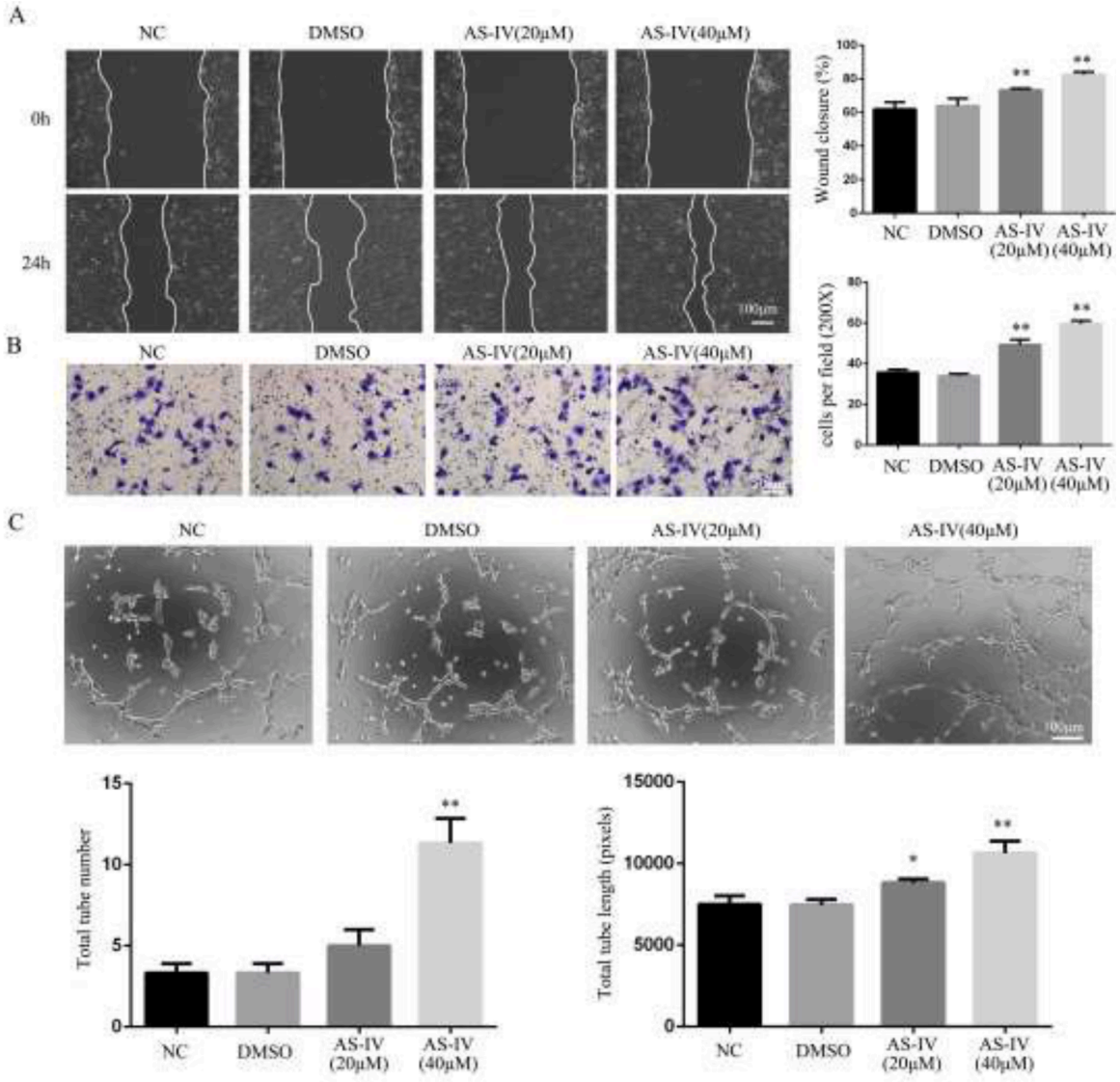

Fig. 3. Effects of AS-IV-treated ADSC-conditioned medium on HUVEC recruitment and Matrigel angiogenesis. (A) Photographs of HUVEC scratch closure after culture with CM from ADSCs treated with 20 μM and 40 μM of AS-IV. The quantitative results are shown on the right side. (B) Photographs of the Transwell experiment illustrate HUVEC recruitment of ADSC CM after treatment with 20 μM and 40 μM of AS-IV. Quantitative results of cell migration are shown on the right side. (C) Representative images of Matrigel tube formation potential from different CMs. The histograms below count the number of tubes and total length of different groups. * $p < 0.05$ and ** $p < 0.01$ *vs*. NC group. All the experiments were repeated three times.

SB225002 inhibits the promotion of ADSC migration and angiogenesis due to high expression of CXCR2

To verify the effect of highly expressed CXCR2 on ADSCs, we added SB225002, a CXCR2 antagonist, at a concentration of 400 nM 1 hour before AS-IV treatment to antagonize CXCR2. The results showed that SB225002 significantly reduced the migration of ADSCs caused by AS-IV (Fig. 5A and 5B) and recruitment of HUVECs (Fig. 5C and 5D), and there was also a small inhibitory effect in the group treated with SB225005 alone. Consistent with the migration study, SB225005 also inhibited the angiogenesis of ADSCs caused by AS-IV (Fig. 5E). At the protein level, SB225002 successfully inhibited the phosphorylation of FAK induced by AS-IV treatment and its downstream p-PXN and β-Catenin expression (Fig. 5F).

The inhibition of FAK phosphorylation by PF573228 plays a negative role in the migration and angiogenesis of ADSCs

To verify the relationship between FAK phosphorylation and CXCR2 expression, we used PF573228 at a concentration of 1 μM to inhibit FAK phosphorylation 1 hour before AS-IV treatment. The results also showed that the migration of ADSCs and the recruitment of HUVECs were inhibited compared with the control group. Similarly, in the AS-IV treatment group, the inhibitor also reduced its promotion of ADSC migration (Fig. 6A and 6B) and the recruitment of HUVECs (Fig. 6C and 6D). This phenomenon was also demonstrated in the tubule formation experiment (Fig. 6E). In subsequent experiments, we analyzed the effect of PF573228 on the protein level, and the results showed that PF573228 did not affect the increase in CXCR2 expression induced by AS-IV, further showing that FAK is activated downstream of CXCR2. The expression of p-PXN and β-Catenin was downregulated as FAK phosphorylation was also inhibited (Fig. 6F).

AS-IV-pretreated ADSCs demonstrate vasculogenic potential in vivo

Subsequently, we used a Matrigel plug assay to demonstrate the in vivo angiogenesis potential of ADSCs after AS-IV pretreatment. ADSCs and ADSCs pretreated with 20 μM or 40 μM AS-IV for 48 h were mixed

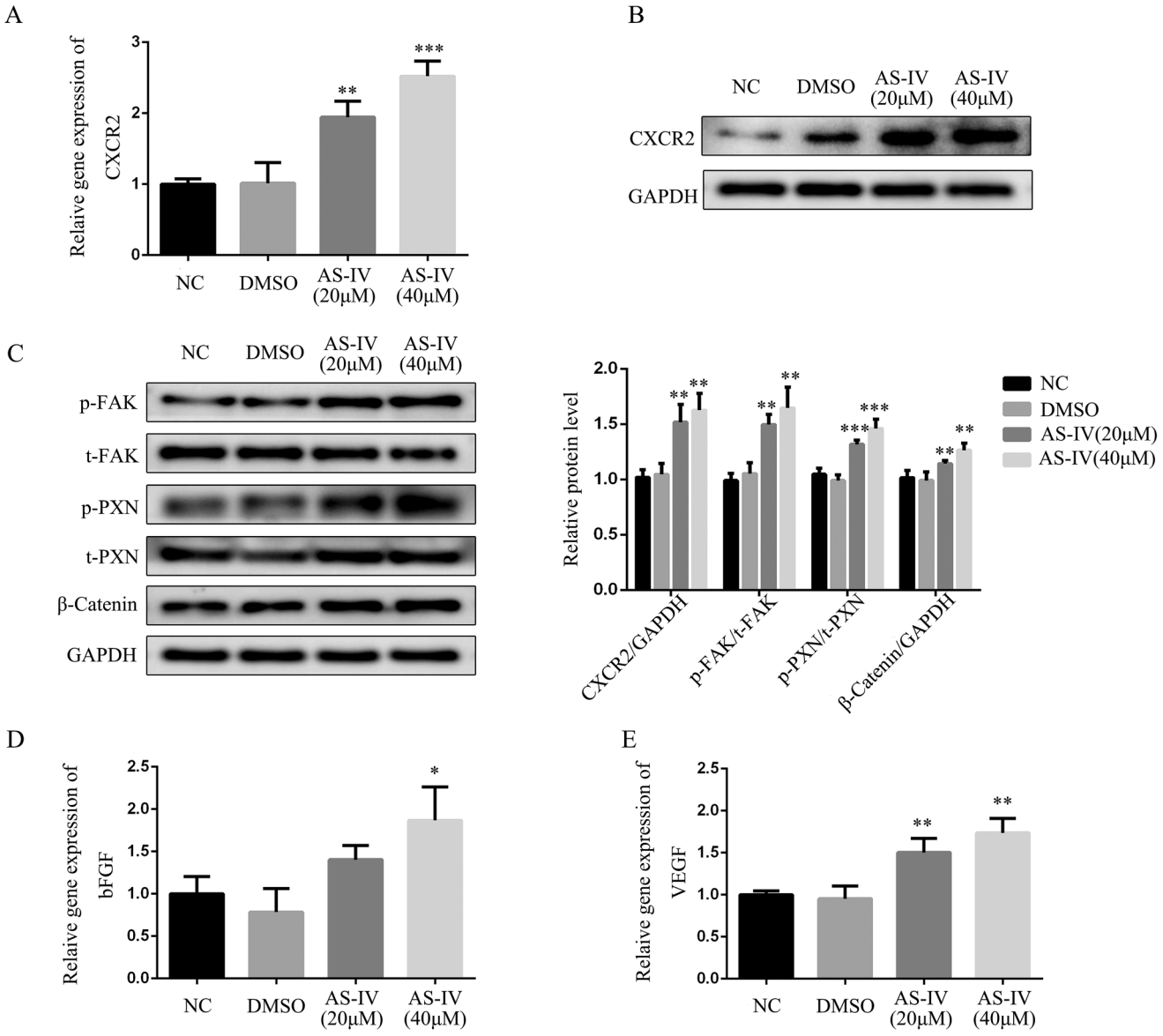

Fig. 4. AS-IV mediated concentration-dependent effects on CXCR2, p-FAK, p-PXN and β-Catenin protein expression and mRNA expression of angiogenesis-related factors. (A) Quantitative RT–PCR analysis of CXCR2 mRNA levels in ADSCs and ADSCs pretreated with AS-IV (20 μM and 40 μM) or DMSO. (B) Western blot analysis of CXCR2 expression in each group. GAPDH was used as a control. (C) Western blot analysis of p-FAK, t-FAK, p-PXN, t-PXN and β-Catenin expression in each group. GAPDH was used as a control, and quantitative results of the relative protein level are shown on the right side. (D) Quantitative RT–PCR analysis of the mRNA levels of the angiogenesis-related factors bFGF and VEGF in each group. * $p < 0.05$ and ** $p < 0.01$ and *** $p < 0.001$ *vs*. the NC group. All the experiments were repeated three times.

with 450 μl Matrigel at a concentration of 5×10^5 cells/50 μl PBS (50 μl PBS mixed with 450 μl Matrigel as a negative control group) and injected into C57BL/6 mice subcutaneously with a syringe. After 2 weeks, the Matrigel plug was recovered and the relative content of hemoglobin was measured using a Drabkin kit. The results showed that ADSCs pretreated with 40 μM AS-IV formed more functional blood vessels in Matrigel (Fig. 7A) and had higher hemoglobin content (Fig. 7B). To confirm that ADSCs demonstrate vasculogenic potential in Matrigel plugs, we sliced and stained Matrigel plugs. H&E staining showed that the Matrigel injected with PBS did not contain typical microvascular-like structures, the formation of microvascular-like structures occurred in the ADSC group, and the ADSC/AS-IV (40 μM) group showed numerous microvascular-like structures (Fig. 7C). Immunofluorescence staining also reflected the increase in the positive area of CD31 in the ADSC/AS-IV (40 μM) group (Fig. 7D).

AS-IV pretreated ADSCs demonstrate therapeutic effects on hind limb ischemia

We further explored the therapeutic effects of ADSCs in a mouse hindlimb ischemia model. After ligation and resection of the left femoral artery for 24 h, 1×10^6 ADSC cells or PBS was injected into the ischemic hindlimb area, and limb blood perfusion was detected by the laser Doppler perfusion index on Days 0, 3, 7, 14 and 21. The results showed that the blood perfusion rate of the limbs injected with ADSCs/AS-IV was higher than the blood perfusion rate of the limbs injected with ADSCs from Day 7 (Fig. 8A and 8B) and increased in concentration gradient. After 28 days, we separated the muscle tissue on the ischemic side, sliced it for immunofluorescence staining, and found that the vascular endothelial cell marker CD31 in the muscles of the ADSC/AS-IV (40 μM) group was significantly increased (Fig. 8C and 8D). We also generated the same model and separated the ischemic muscle specimens

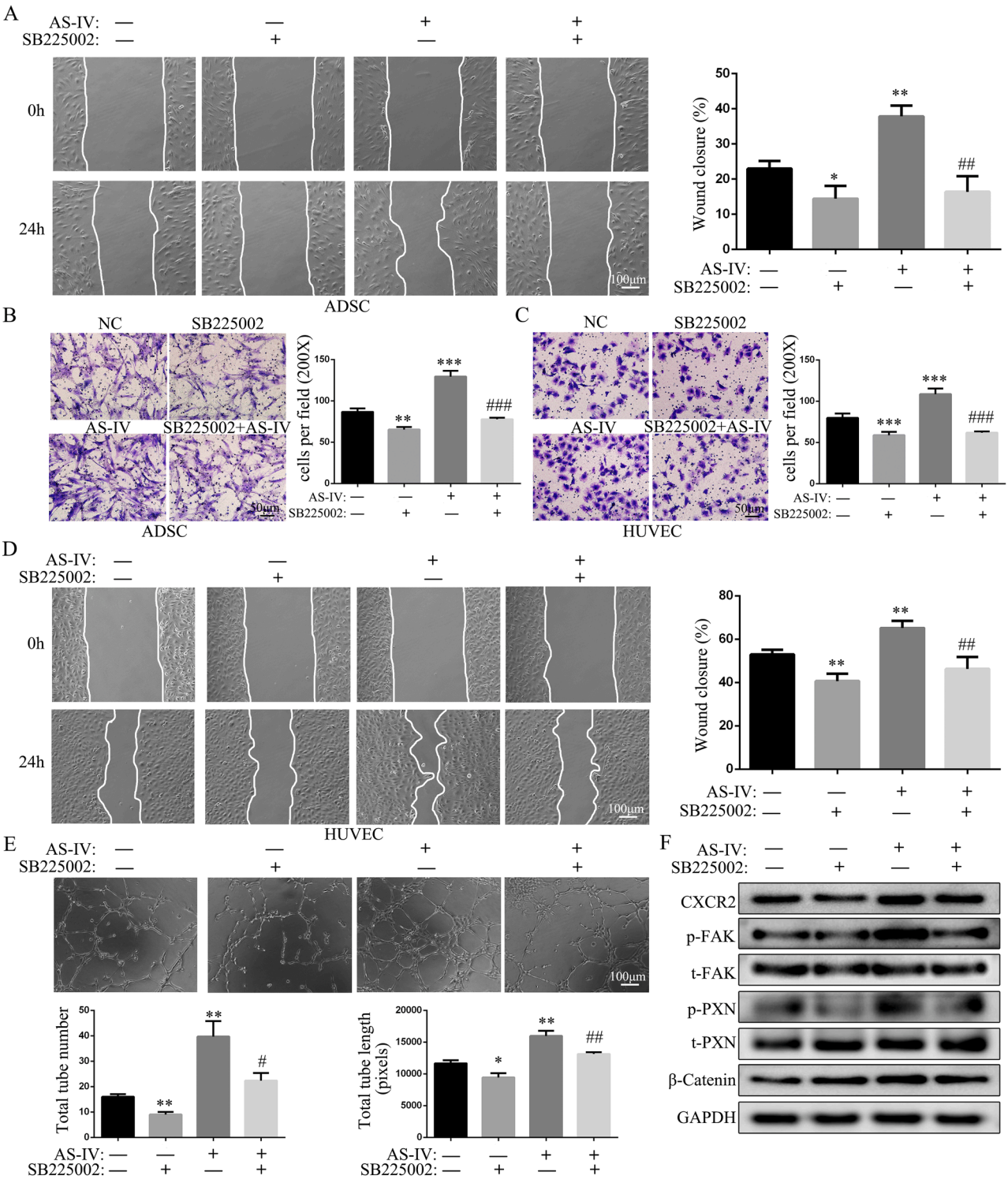

Fig. 5. SB225002 inhibited the increase in migration and angiogenesis of ADSCs induced by CXCR2 overexpression. (A) After preincubation with SB225002 (1 μM) for 1 h, ADSCs were treated with 40 μM AS-IV for 48 h, and a wound healing assay was used to evaluate the healing ability. Quantitative results are shown on the right side. (B) Transwell assay to evaluate the migration ability of ADSCs treated with 40 μM AS-IV after preincubation with SB225002 or not, and quantify the number of cells passed. (C) Transwell assay to evaluate the recruitment effect on HUVECs in ADSC CMs. ADSCs were pretreated with 40 μM AS-IV and SB225002, and quantitative results are shown on the right side. (D) Wound healing assay to evaluate the healing ability of HUVECs treated with different CMs. Quantitative of wound closure is shown on the right side. (E) Representative images of Matrigel tube formation potential from different CMs. The histograms below count the number of tubes and total length of different groups. (F) After preincubation with SB225002 or 40 μM AS-IV, ADSCs were subjected to Western blots and detected with the indicated antibodies.* $p < 0.05$, ** $p < 0.01$ and *** $p < 0.001$ *vs.* the control group. # $p < 0.05$, ## $p < 0.01$ and ### $p < 0.001$ *vs.* the AS-IV group. All the experiments were repeated three times.

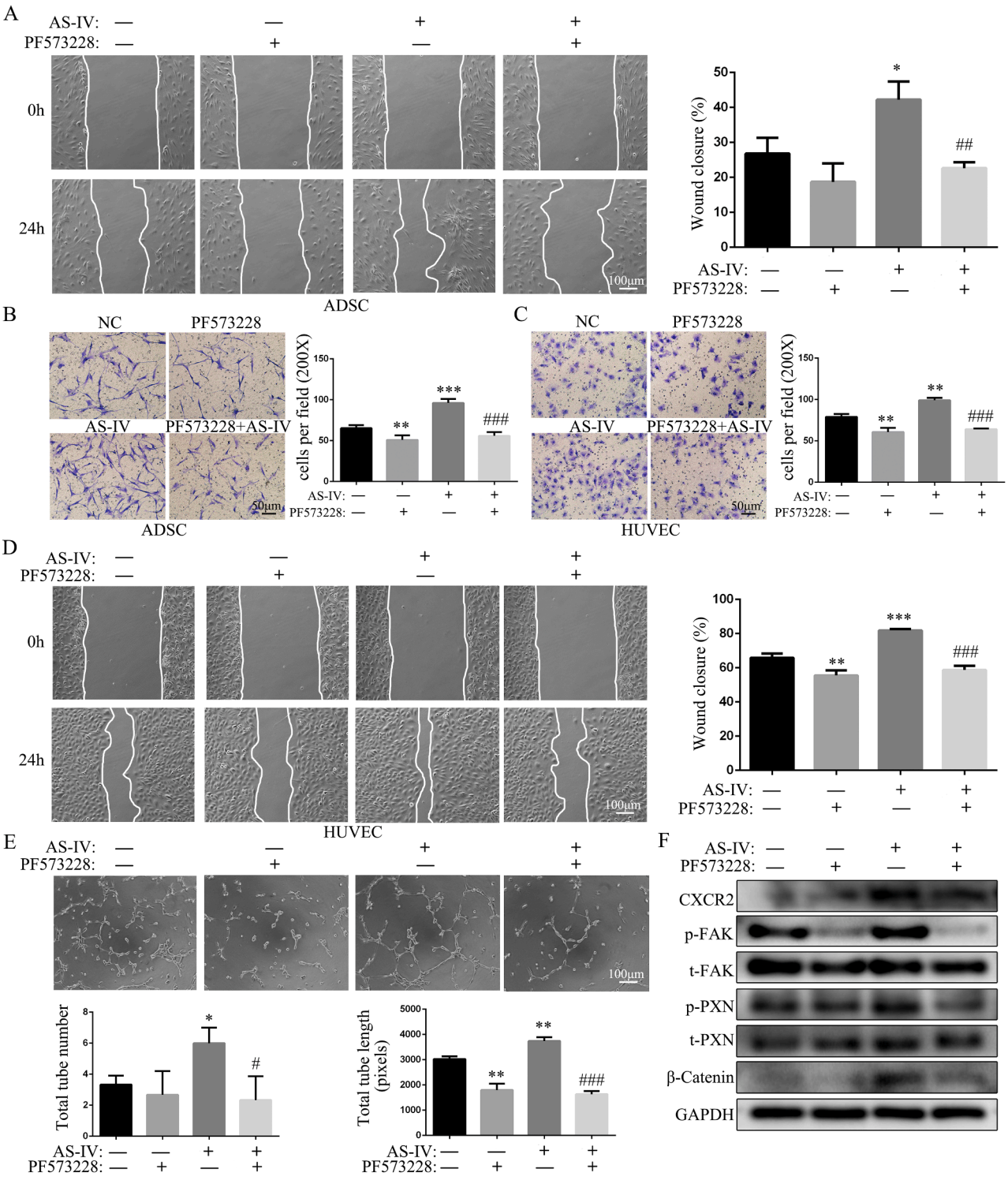

Fig. 6. Effect of the FAK phosphorylation inhibitor PF573228 on ADSC migration and angiogenesis ability. (A) After preincubation with PF573228 (10 μM) for 1 h, ADSCs were treated with 40 μM AS-IV for 48 h and a wound healing assay was used to evaluate the healing ability. Quantitative results are shown on the right side. (B) Transwell assay to evaluate the migration ability of ADSCs treated with 40 μM AS-IV after preincubation with PF573228 or not and quantify the number of cells passed. (C) Transwell assay to evaluate the recruitment effect on HUVECs in ADSC CMs. ADSCs were pretreated with 40 μM AS-IV and PF573228, and quantitative results are shown on the right side. (D) Wound healing assay to evaluate the healing ability of HUVECs treated with different CMs. Quantitative wound closure is shown on the right side. (E) Representative images of Matrigel tube formation potential from different CMs. The histograms below count the number of tubes and total length of different groups. (F) After preincubation with PF573228 or 40 μM AS-IV, ADSCs were subjected to Western blots and detected with the indicated antibodies.* $p < 0.05$, ** $p < 0.01$ and *** $p < 0.001$ *vs.* the control group. # $p < 0.05$, ## $p < 0.01$ and ### $p < 0.001$ *vs.* the AS-IV group. All the experiments were repeated three times.

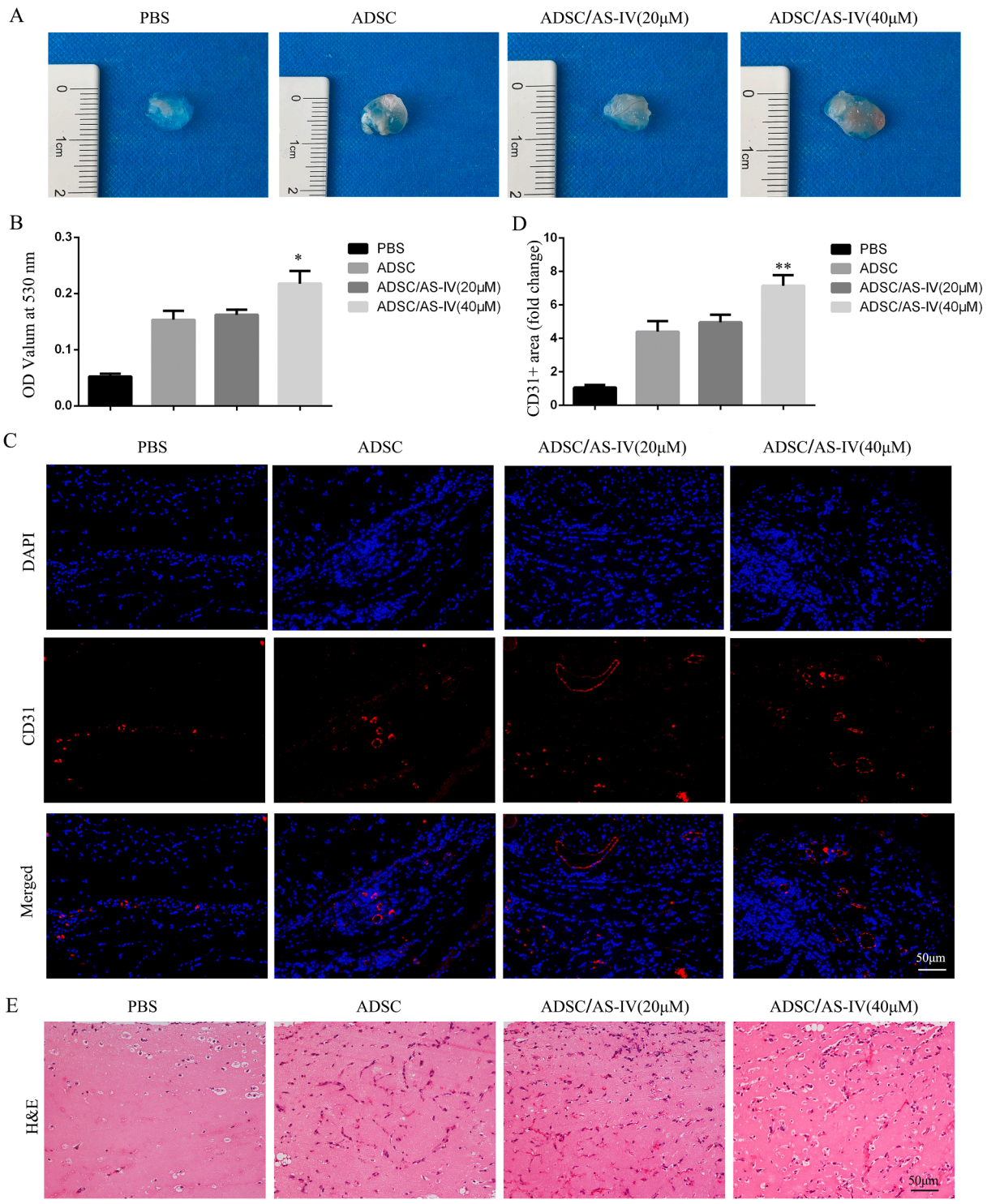

Fig. 7. Vasculogenic potential *in vivo* measured by Matrigel plug assay. (A) Representative photographs of Matrigel plugs injected with PBS, ADSCs or ADSC pretreated with 20 μM or 40 μM AS-IV at Day 14. (B) OD value of hemoglobin concentration in Matrigel plug. (C) Immunofluorescent staining of CD31 in sections of Matrigel plugs. (D) Quantification of the CD31+ area was performed. (E) H&E-stained sections of Matrigel plug.* $p < 0.05$ and ** $p < 0.01$ *vs.* ADSC group. All the experiments were repeated three times.

after 14 days of cytotherapy for H&E staining to observe the inflammatory response and muscle necrosis in the early stage of ischemic recovery. The results showed that the PBS group had severe muscle damage, accompanied by obvious inflammation infiltration and fibrosis, and the intermuscular space was blurred, while inflammation and muscle degeneration were reduced in the ADSC group, and the reduction was more significant in the ADSC/AS-IV (40 μM) group (Fig. 8E).

Discussion

CLI is a serious form of peripheral arterial disease. In recent years, ADSCs transplantation has become one of the effective treatment methods for CLI patients who are not suitable for surgery. Unlike other mesenchymal stem cells, ADSCs are easier to obtain and have fewer ethical problems (Ai et al., 2016; Jaluvka et al., 2020). However, the

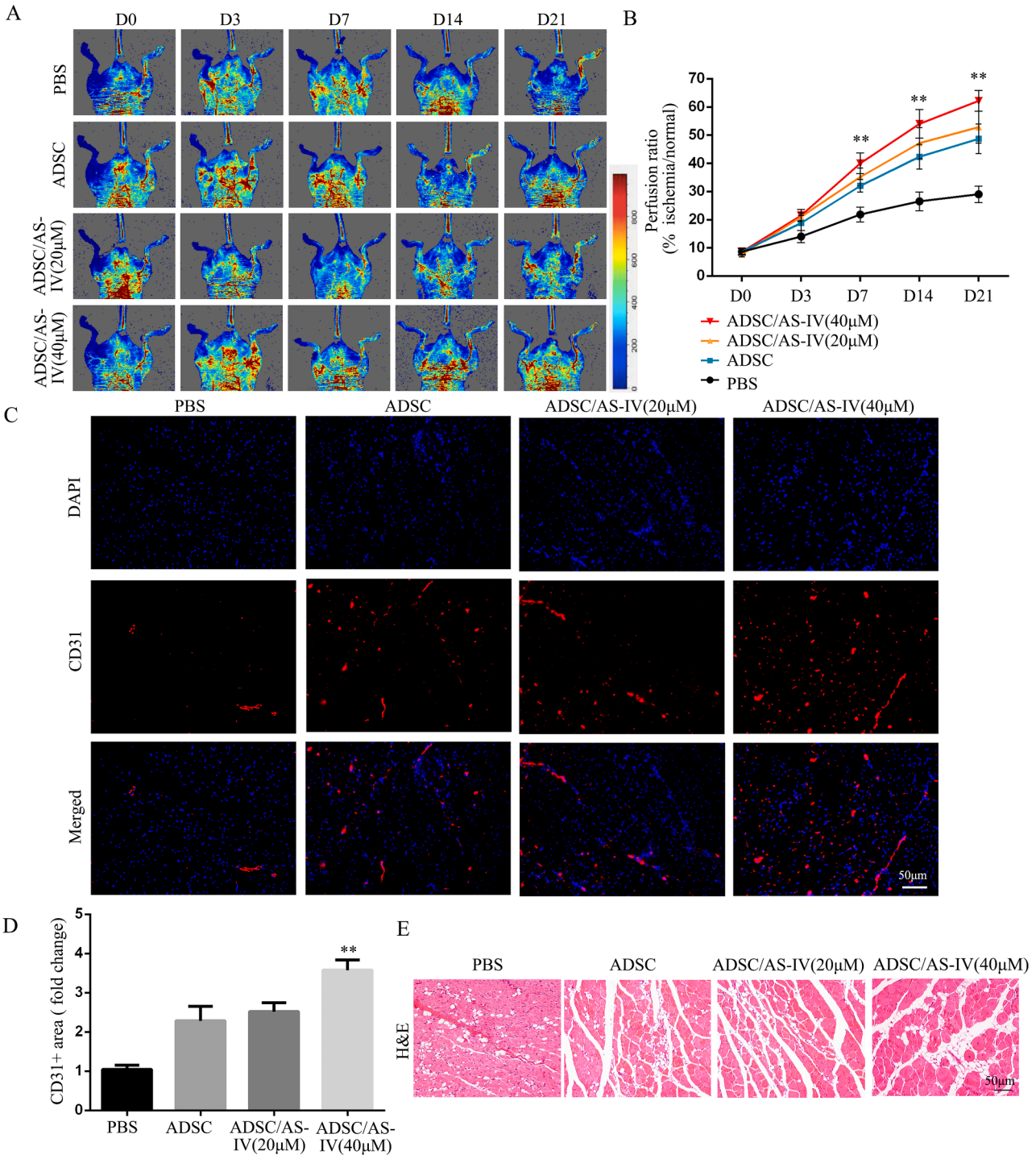

Fig. 8. Recovery of blood flow and therapeutic mechanism in a mouse model of hind limb ischemia after cell transplantation. (A) Representative laser Doppler perfusion images of the recovery of blood flow in ischemic hind limbs 21 days after intramuscular injection with PBS, ADSCs, ADSCs/AS-IV (20 μM) and ADSCs/AS-IV (40 μM). (B) Blood perfusion ratio between different groups in 21 days. (C) Immunofluorescent staining for CD31 in sections of gastrocnemius tissue sections at Day 21. (D) The proportion of CD31+ area in each group. (E) H&E-stained sections of gastrocnemius tissue sections at Day 14. ** $p < 0.01$ *vs.* ADSC group. All the experiments were repeated three times.

therapeutic effect of ADSCs is still limited, because of the weak biological activity or poor migration ability of cells (Eggenhofer et al., 2012), the injected ADSCs will be consumed in large quantities due to the ischemic and hypoxic environment at the injection site. Therefore, increasing the activity of ADSCs is an important method to improve the success rate of cytotherapy.

Astragaloside IV, a natural plant extract, has been shown to have cardiovascular protective effects (Ma et al., 2013) and can reduce endothelial dysfunction related to diabetes and its complications. In a study of its effect on HUVECs, AS-IV was found to be able to promote endothelial cell proliferation and reduce hypoxia damage (Cheng et al., 2019; Wang et al., 2013). In this study, we pretreated ADSCs with AS-IV and found that AS-IV could improve the migration ability, HUVEC recruitment and angiogenesis ability of ADSCs *in vitro*. According to previous studies, the homing ability of ADSCs helps them navigate to the damage site, and migration and surface molecule-mediated adhesion are

the core mechanisms of the homing process (Nitzsche et al., 2017). That is, AS-IV can enhance the therapeutic effect by promoting the homing ability of ADSCs. At the same time, endothelial cells migration ability and remodeling into tubular structures are also crucial for angiogenesis. In this process, many different cytokines are involved in regulating the migration of chemotactic endothelial cells in angiogenesis, such as VEGF, bFGF and angiopoietin (Lamalice et al., 2007). Due to the effect of AS-IV, the ability of ADSCs to recruit endothelial cells is also greatly increased, and the vascularization ability is also enhanced accordingly. *In vivo* experiments further verified the therapeutic effect of AS-IV pretreated ADSCs on hindlimb ischemia. The Matrigel plug assay showed that the ADSC/AS-IV group resulted in better formation of the vascular network and more hemoglobin penetration. The immunofluorescence experiment also showed more CD31+ vascular endothelium in the AS-IV pre-treated group, which can fully reflected the angiogenesis potential *in vivo* (Chambers et al., 2021). In the ischemic hindlimb mice model, AS-IV pretreated ADSCs had better hindlimb blood flow recovery from the 7th day of treatment. Tissue sections also reflect the higher capillary density in AS-IV pretreated group, and there were less inflammatory infiltration and muscle degeneration in ADSC/AS-IV group in H & E staining. It may suggest that the ADSC after AS-IV treatment can better change the microenvironment around the injection site, exert a stronger anti-inflammatory effect, and reduce the damage to muscle cells. As the capillary density in the treated area increases, a better blood supply can also lead tobetter muscle fiber repair (Jacobsen et al., 2021).

In view of the role of AS-IV in ADSCs, we focused our attention on the chemokine system, which is closely related to cell movement and recruitment. Chemokines and their receptors have been found to play an important role in tissue ischemia repair, not only in the recruitment of macrophages and endothelial cells but also in enhancing the proliferation of myoblasts. The major groups of chemokines and their receptors related to angiogenesis are CXCL1, CXCL2, CXCL3, CXCL5, CXCL6, CXCL7, CXCL8/CXCR2 and CXCL12/CXCR4 (Shireman, 2007). Previous study also showed that AS-IV apparently promotes CXCR2 expression on LPS-induced neutrophils (Huang et al., 2016). Thus, we screened these chemokines and their receptors by qRT–PCR and found that after AS-IV treatment, the expression of CXCR2 and CXCR4 in ADSCs increased significantly with the concentration gradient. After using their receptor antagonists (Fig. 7 and Fig. S2), we found that although many previous studies have verified the positive role of CXCR4 in stem cell migration and the therapeutic effect (Li et al., 2017), in this study, CXCR2, but not CXCR4, played a key role. CXCR2 is an important chemokine receptor that mediates cell chemotaxis. CXCR2 is related to inflammatory diseases and immune responses. The upregulation of CXCR2 is also related to tumor angiogenesis and tumor metastasis and can trigger PI3K/Akt, MAPK and other signaling cascades (Yang et al., 2010). In this experiment, we found that the overexpression of CXCR2 led to the activation of FAK/PXN and the upregulation of β-Catenin. Many studies have shown that FAK can be used as an upstream regulator to regulate the expression of β-Catenin (Barnawi et al., 2020), and it can also promote cell migration by forming FAK/Src complexes, activating PI3K, and regulating the Rho subfamily. At the same time, FAK kinase activity and its autophosphorylation at Y397 are also considered necessary for normal vascular development (Zhao and Guan, 2011). PXN, as a cytoskeletal protein located in focal adhesion and related to cell adhesion, is phosphorylated by FAK at its tyrosine residue at position 118 to participate in cell adhesion and metastasis (Chen et al., 2012). Studies have confirmed that under the control of the Tie2 promoter and enhancer, transgenic expression of ectopic FAK in endothelial cells increases angiogenesis in hindlimb ischemia and wound-induced angiogenesis models (Peng et al., 2004). Previous study also found that after aquaporin 1 overexpression, FAK and β-Catenin ware upregulated, which improved the endothelial adhesion characteristics of MSCs and then enhanced migration (Meng et al., 2014), which was also consistent with our findings. To verify the effect of FAK activation on angiogenesis, we used the FAK phosphorylation inhibitor PF573228 to pretreat ADSCs and found that after using PF573228, the migration and angiogenesis of ADSCs promoted by AS-IV was inhibited, the expression of p-PXN and β-Catenin was reduced, and the expression of CXCR2 was not affected, further indicating that CXCR2, as an upstream factor, promotes the activation of FAK and then affects the migration and angiogenesis of ADSCs.

Collectively, our findings illustrated that AS-IV pretreated ADSCs exhibit stronger migration and angiogenesis capabilities, and have better therapeutic function for hindlimb ischemia. Mechanistically, AS-IV promotes the expression of CXCR2 in ADSCs, leading to the phosphorylation of FAK, which in turn plays a key role. This may bring new insights into the treatment of critical limb ischemia. However, the specific mechanism of action may require further molecular biology experiments, and further investigation through clinical studies to test the long-term safety and effectiveness of this method.

Author contributions

Weiyi Wang, Zekun Shen and Yanan Tang performed the experiments. Bingyi Chen, Jinxing Chen, and Jiaxuan Hou analyzed and interpreted the data. Shaoying Lu and Weiyi Wang wrote the manuscript. Jiayan Li and Mengzhao Zhang provided critical suggestions. Shuang Liu, Yifan Mei and Liwei Zhang revised the manuscript critically for important intellectual content. Shaoying Lu designed and supervised the project. All data were generated in-house, and no paper mill was used. All authors agree to be accountable for all aspects of work ensuring integrity and accuracy.

Credit author statement

Weiyi Wang: Experiment Operation, Data Curation, Writing - Original Draft **Zekun Shen:** Experiment Operation, Formal analysis **Yanan Tang:** Experiment Operation **Bingyi Chen:** Validation **Jinxing Chen:** Validation **Jiaxuan Hou:** Validation **Jiayan Li:** Conceptualization **Mengzhao Zhang:** Conceptualization **Shuang Liu:** Writing - Review & Editing **Yifan Mei:** Writing - Review & Editing **Liwei Zhang:** Writing - Review & Editing **Shaoying Lu:** Conceptualization, Writing - Review & Editing, Supervision, Project administration, Funding acquisition

Funding

This work was supported by the National Natural Science Foundation of China (No: 81472747).

Availability of data and materials

The datasets generated/analyzed during the current study are available.

Ethics approval and consent to participate

This study was approved and supervised by the Ethical Committee of The First Affiliated Hospital of Medical College, Xi'an Jiaotong University, Xi'an, China (Approval number: 2021–1568, Approval date: May 6, 2021). The study was conducted in accordance with the Declaration of Helsinki principles.

Consent for publication

The manuscript has been approved by all authors for publication.

Declaration of Competing Interest

The authors declare no conflict of interest.

Acknowledgments

We thank the Department of Pharmacy of the Air Force Medical University of China for their help with the laser Doppler instrument and appreciate our colleagues for their valuable efforts and comments on this paper.

Supplementary materials

Supplementary material associated with this article can be found, in the online version, at doi:10.1016/j.phymed.2021.153908.

References

Ai, M., Yan, C.F., Xia, F.C., Zhou, S.L., He, J., Li, C.P., 2016. Safety and efficacy of cell-based therapy on critical limb ischemia: a meta-analysis. Cytotherapy 18 (6), 712–724.

Barnawi, R., Al-Khaldi, S., Bakheet, T., Fallatah, M., Alaiya, A., Ghebeh, H., Al-Alwan, M., 2020. Fascin activates beta-catenin signaling and promotes breast cancer stem cell function mainly through focal adhesion kinase (FAK): relation with disease progression. Front. Oncol. 10.

Beltran-Camacho, L., Rojas-Torres, M., Duran-Ruiz, M.C., 2021. Current status of angiogenic cell therapy and related strategies applied in critical limb ischemia. Int. J. Mol. Sci. 22 (5).

Campia, U., Gerhard-Herman, M., Piazza, G., Goldhaber, S.Z., 2019. Peripheral artery disease: past, present, and future. Am. J. Med. 132 (10), 1133–1141.

Chambers, S.E.J., Pathak, V., Pedrini, E., Soret, L., Gendron, N., Guerin, C.L., Stitt, A.W., Smadja, D.M., Medina, R.J., 2021. Current concepts on endothelial stem cells definition, location, and markers. Stem Cells Transl. Med. 10 (Suppl 2), S54–S61.

Chen, T.C., Lai, C.H., Chang, J.L., Chang, S.W., 2012. Mitomycin C retardation of corneal fibroblast migration via sustained dephosphorylation of paxillin at tyrosine 118. Invest. Ophthalmol. Vis. Sci. 53 (3), 1539–1547.

Cheng, S., Zhang, X., Feng, Q., Chen, J., Shen, L., Yu, P., Yang, L., Chen, D., Zhang, H., Sun, W., Chen, X., 2019. Astragaloside IV exerts angiogenesis and cardioprotection after myocardial infarction via regulating PTEN/PI3K/Akt signaling pathway. Life Sci. 227, 82–93.

Eggenhofer, E., Benseler, V., Kroemer, A., Popp, F.C., Geissler, E.K., Schlitt, H.J., Baan, C. C., Dahlke, M.H., Hoogduijn, M.J., 2012. Mesenchymal stem cells are short-lived and do not migrate beyond the lungs after intravenous infusion. Front. Immunol. 3, 297.

Feng, B., Zhang, Q., Wang, X., Sun, X., Mu, X., Dong, H., 2017. Effect of andrographolide on gene expression profile and intracellular calcium in primary rat myocardium microvascular endothelial cells. J. Cardiovasc. Pharmacol. 70 (6), 369–381.

Huang, P., Lu, X., Yuan, B., Liu, T., Dai, L., Liu, Y., Yin, H., 2016. Astragaloside IV alleviates E. coli-caused peritonitis via upregulation of neutrophil influx to the site of infection. Int. Immunopharmacol. 39, 377–382.

Hutchings, G., Janowicz, K., Moncrieff, L., Dompe, C., Strauss, E., Kocherova, I., Nawrocki, M.J., Kruszyna, L., Wasiatycz, G., Antosik, P., Shibli, J.A., Mozdziak, P., Perek, B., Krasinski, Z., Kempisty, B., Nowicki, M., 2020. The proliferation and differentiation of adipose-derived stem cells in neovascularization and angiogenesis. Int. J. Mol. Sci. 21 (11).

Jacobsen, N.L., Norton, C.E., Shaw, R.L., Cornelison, D.D.W., Segal, S.S., 2021. Myofibre injury induces capillary disruption and regeneration of disorganized microvascular networks. J. Physiol.

Jaluvka, F., Ihnat, P., Madaric, J., Vrtkova, A., Janosek, J., Prochazka, V., 2020. Current status of cell-based therapy in patients with critical limb ischemia. Int. J. Mol. Sci. 21 (23).

Jiang, B., Yang, Y.J., Dang, W.Z., Li, H., Feng, G.Z., Yu, X.C., Shen, X.Y., Hu, X.G., 2020. Astragaloside IV reverses simvastatin-induced skeletal muscle injury by activating the AMPK-PGC-1alpha signalling pathway. Phytother. Res. 34 (5), 1175–1184.

Lamalice, L., Le Boeuf, F., Huot, J., 2007. Endothelial cell migration during angiogenesis. Circ. Res. 100 (6), 782–794.

Li, M.W., Sun, X.F., Ma, L., Jin, L., Zhang, W.F., Xiao, M., & Yu, Q., 2017. SDF-1/CXCR4 axis induces human dental pulp stem cell migration through FAK/PI3K/Akt and GSK3 beta/beta-catenin pathways. Sci. Rep.. 7.

Li, X.L., Gan, K.X., Song, G.Y., Wang, C., 2015. VEGF gene transfected umbilical cord mesenchymal stem cells transplantation improve the lower limb vascular lesions of diabetic rats. J. Diabetes Complicat. 29 (7), 872–881.

Liew, A., O'Brien, T., 2012. Therapeutic potential for mesenchymal stem cell transplantation in critical limb ischemia. Stem Cell Res. Ther. 3 (4), 28.

Limbourg, A., Korff, T., Napp, L.C., Schaper, W., Drexler, H., Limbourg, F.P., 2009. Evaluation of postnatal arteriogenesis and angiogenesis in a mouse model of hind-limb ischemia. Nat. Protoc. 4 (12), 1737–1746.

Lu, H.Y., Wang, F., Mei, H., Wang, S.Q., Cheng, L.M., 2018. Human adipose mesenchymal stem cells show more efficient angiogenesis promotion on endothelial colony-forming cells than umbilical cord and endometrium. Stem. Cells Int. 2018.

Ma, X., Zhang, K., Li, H., Han, S., Ma, Z., Tu, P., 2013. Extracts from Astragalus membranaceus limit myocardial cell death and improve cardiac function in a rat model of myocardial ischemia. J. Ethnopharmacol. 149 (3), 720–728.

Meng, F.B., Rui, Y.F., Xu, L.L., Wan, C., Jiang, X.H., Li, G., 2014. Aqp1 enhances migration of bone marrow mesenchymal stem cells through regulation of FAK and beta-Catenin. Stem. Cells Dev. 23 (1), 66–75.

Min, Y., Han, S., Aae Ryu, H., Kim, S.W., 2018. Human adipose mesenchymal stem cells overexpressing dual chemotactic gene showed enhanced angiogenic capacity in ischaemic hindlimb model. Cardiovasc. Res. 114 (10), 1400–1409.

Nitzsche, F., Muller, C., Lukomska, B., Jolkkonen, J., Deten, A., Boltze, J., 2017. Concise review: MSC adhesion cascade-insights into homing and transendothelial Migration. Stem Cells 35 (6), 1446–1460.

Orciani, M., Di Primio, R., 2013. Skin-derived mesenchymal stem cells: isolation, culture, and characterization. Methods Mol. Biol. 989, 275–283.

Peng, X., Ueda, H., Zhou, H.M., Stokol, T., Shen, T.L., Alcaraz, A., Nagy, T., Vassalli, J.D., Guan, J.L., 2004. Overexpression of focal adhesion kinase in vascular endothelial cells promotes angiogenesis in transgenic mice. Cardiovasc. Res. 64 (3), 421–430.

Potdar, P.D., Jethmalani, Y.D., 2015. Human dental pulp stem cells: applications in future regenerative medicine. World J. Stem Cells 7 (5), 839–851.

Shireman, P.K., 2007. The chemokine system in arteriogenesis and hind limb ischemia. J. Vasc. Surg. 45 (Suppl A), A48–A56.

Tateishi-Yuyama, E., Matsubara, H., Murohara, T., Ikeda, U., Shintani, S., Masaki, H., Amano, K., Kishimoto, Y., Yoshimoto, K., Akashi, H., Shimada, K., Iwasaka, T., Imaizumi, T., 2002. Therapeutic angiogenesis for patients with limb ischaemia by autologous transplantation of bone-marrow cells: a pilot study and a randomised controlled trial. Lancet 360 (9331), 427–435.

Wang, S.G., Xu, Y., Chen, J.D., Yang, C.H., Chen, X.H., 2013. Astragaloside IV stimulates angiogenesis and increases nitric oxide accumulation via JAK2/STAT3 and ERK1/2 pathway. Molecules 18 (10), 12809–12819.

Xu, F., Cui, W.Q., Wei, Y., Cui, J., Qiu, J., Hu, L.L., Gong, W.Y., Dong, J.C., Liu, B.J., 2018. Astragaloside IV inhibits lung cancer progression and metastasis by modulating macrophage polarization through AMPK signaling. J. Exp. Clin. Cancer Res. 37 (1), 207.

Yang, G., Rosen, D.G., Liu, G.Z., Yang, F., Guo, X.Q., Xiao, X., Xue, F.X., Mercado-Uribe, I., Huang, J.T., Lin, S.H., Mills, G.B., Liu, J.S., 2010. CXCR2 Promotes ovarian cancer growth through dysregulated cell cycle, diminished apoptosis, and enhanced angiogenesis. Clin. Cancer Res. 16 (15), 3875–3886.

Zhang, L., Liu, Q., Lu, L., Zhao, X., Gao, X., Wang, Y., 2011. Astragaloside IV stimulates angiogenesis and increases hypoxia-inducible factor-1alpha accumulation via phosphatidylinositol 3-kinase/Akt pathway. J. Pharmacol. Exp. Ther. 338 (2), 485–491.

Zhao, X., Guan, J.L., 2011. Focal adhesion kinase and its signaling pathways in cell migration and angiogenesis. Adv. Drug Deliv. Rev. 63 (8), 610–615.

Zuk, P.A., Zhu, M., Ashjian, P., De Ugarte, D.A., Huang, J.I., Mizuno, H., Alfonso, Z.C., Fraser, J.K., Benhaim, P., Hedrick, M.H., 2002. Human adipose tissue is a source of multipotent stem cells. Mol. Biol. Cell 13 (12), 4279–4295.